Full control modes of three-wheeled vehicles with zero body sideslip angle and zero body motions

C-C Yu[1*] and **T Liu**[2]
[1]Department of Vehicle Engineering, National Taipei University of Technology, Taipei, Taiwan
[2]Department of Mechanical Engineering, National Taiwan University, Taipei, Taiwan

Abstract: By using the full control concept, zero body sideslip angle and zero body motions can be achieved. In this study, firstly, the governing equations for the six-degree-of-freedom three-wheeled vehicle model, with either two wheels on the front axle or two wheels on the rear axle are developed. With six properly chosen control inputs, there are nine full control modes for the zero body sideslip angle and zero body motion control. The sum of tractive forces, cornering forces or active suspension forces is set as the criterion for evaluating these full control modes. These control modes are compared and discussed for typical driving scenarios, and conclusions are drawn about preferable modes.

Keywords: full control, zero body sideslip angle, zero body motions, vehicle dynamics

Notation

b	wheel track
c	longitudinal distance between CG and mass centre of sprung body
$C_{\phi i}$	damping coefficient of ith wheel
CG	centre of gravity
e	longitudinal distance between CG and mass centre of unsprung body
f	longitudinal distance between CG and pitch axis
F_{wx}	vehicle aerodynamic drag
F_{xi}	tractive force on ith wheel
F_{xl}	tractive force on left-side wheel
F_{xr}	tractive force on right-side wheel
F_{xs}	tractive force on singled wheel
F_{yi}	cornering force on ith wheel
F_{zi}	active suspension force on ith wheel
F_{zl}	active suspension force on left-side wheel
F_{zr}	active suspension force on right-side wheel
F_{zs}	active suspension force on singled wheel
h_s	vertical distance between CG and mass centre of sprung body
h_ϕ	vertical distance between roll axis and mass centre of sprung body
H_x	roll angular momentum of sprung body
H_y	pitch angular momentum of sprung body
H_z	yaw angular momentum of sprung body
$H_{z'}$	yaw angular momentum of unsprung body
I_{xxs}	moment of inertia of sprung body in x direction
I_{xzs}	product of inertia of sprung body
I_{yys}	moment of inertia of sprung body in y direction
I_{zzs}	moment of inertia of sprung body in z direction
I_{zzu}	moment of inertia of unsprung body
k_x	aerodynamic drag factor
$K_{\phi i}$	spring stiffness of ith wheel
l	wheel base
l_f	distance between CG and front axle
l_r	distance between CG and rear axle
M	mass of vehicle
M_s	mass of sprung body
M_u	mass of unsprung body
δ_i	steering angle of ith wheel
δ_f	front steering angle
δ_r	rear steering angle

The MS was received on 17 July 2000 and was accepted after revision for publication on 22 March 2001.
**Corresponding author: Department of Vehicle Engineering, National Taipei University of Technology, 1, Sec. 3, Chung-Hsiao E. Road, Taipei, Taiwan 106.*

1 INTRODUCTION

The motion of a vehicle consists of six components: longitudinal, lateral, bounce, roll, pitch and yaw. It would be ideal if all of the six components of motion can be controlled. Thus, the dynamics of a vehicle can be improved and the manoeuvring of the vehicle can be controlled more precisely within the limitation of its performance. However, to control these six motion components fully, six control inputs are needed and should be selected properly.

In traditional vehicles, the driver uses the steering-wheel to control the steering angle of a set of wheels and the accelerator or the brake pedal to control the longitudinal (tractive or braking) forces of the wheels. Only two control inputs are used to drive the vehicle. Using the traditional steering mechanism could change the vehicle course, yet the lateral and yaw motion of the vehicle cannot be controlled fully. Furthermore, the body motions (i.e. bounce, pitch and roll) of the vehicle cannot be controlled by using the steering-wheel, accelerator or brake pedal. The motion of the vehicle is said to be only partially controlled [**1**].

Various control systems such as four-wheel steering, active suspension, variable torque split four-wheel drive and traction control, as well as anti-lock brakes, have been developed in the recent past [**2–5**]. With the aid of these systems, additional control inputs can be introduced. As the number of input controls increases, the motion of vehicle can be fully controlled.

If each wheel could be steered, and powered or braked, and if also the suspension force of each wheel could be controlled independently, there could be more than six control inputs. A four-wheeled vehicle could have up to twelve control inputs and a three-wheeled vehicle could have up to nine control inputs. Within these control inputs, if six control inputs are properly chosen, the motion of the vehicle with all six components can be fully controlled. This is called full control in this study.

During a turn, the build-up of body sideslip angle delays the vehicle lateral response and retards the vehicle's turning performance [**6**]. Furthermore, the body motions not only increase the passenger's sensation of discomfort but also increase the tyre longitudinal and lateral weight transfer, and sequentially the tyre total cornering force is reduced [**7**, **8**]. Inhibition of the body sideslip and the body motion has significant effects on improving vehicle dynamics, and it is the objective of the control rules developed in the following study.

It is known that four-wheel steering, which combines two steering mechanisms, can reduce the body sideslip angle [**5**, **6**, **9**]. Additionally, using an active suspension system can control the vehicle body attitude and increase the ride comfort effectively [**2–4**].

Abe [**10**] used a two-degree-of-freedom linear bicycle model and a full control concept to establish the control rules of two steering angles (the front and the rear steering angles) in order to control a vehicle negotiating a turn with zero body sideslip angle. Matsumoto and Tomizuka [**11**] built another two-degree-of-freedom full control model, in which two of three steering mechanisms (the front steering angle, rear steering angle and differential tractive force) were chosen as the control inputs.

Yu and Liu [**1**], in order to realize zero body sideslip angle and zero body roll motion control, established a planar three-degree-of-freedom full control model and developed the control rules by combining two of the three steering mechanisms and active suspension forces simultaneously.

This study looks at the dynamics of three-wheeled vehicles with either two wheels on the front axle or two wheels on the rear axle, and presents a full control strategy for selecting control inputs in order to improve the vehicle steering response and decrease tyre dynamic weight transfer while eliminating the lateral velocity and the body motions.

Simplified, yet complete, six-degree-of-freedom models and governing equations for both cases are developed. The control of steering angles, longitudinal forces and active suspension forces of wheels are derived, and the full control concept of the vehicle can be achieved. This model can also be applied to satisfy other driving situations, not just zero body sideslip and zero body motion control.

The criteria for selecting proper control modes are based on practical considerations. A numerical comparison, using typical vehicle data, shows some interesting results for the different control modes. Through the comparisons and discussions, the preferable control modes in different driving scenarios have been chosen.

2 MODELLING

In the model, the steering angle, tractive or braking force, and active suspension force for each wheel are set as the possible individually controllable input parameters. There are nine control inputs for the three-wheeled vehicle. Later on, after the steering angles of the same axle are combined, a total of eight useful control inputs are used in the governing equations.

There are two configurations for the three-wheeled vehicle in this study. One is two wheels on the front axle and is called the 2F1R three-wheeled vehicle; the other is two wheels on the rear axle and is called the 1F2R three-wheeled vehicle, as shown in Fig. 1, where wheels 1, 2 and 3 represent the front-left, front-right and singled rear wheel of the 2F1R three-wheeled vehicle and wheels 4, 5 and 6 represent the singled front, rear-left and rear-right wheel of the 1F2R three-wheeled vehicle.

The vehicle is divided into two parts: sprung and unsprung bodies, as shown in Fig. 2a. The unsprung body

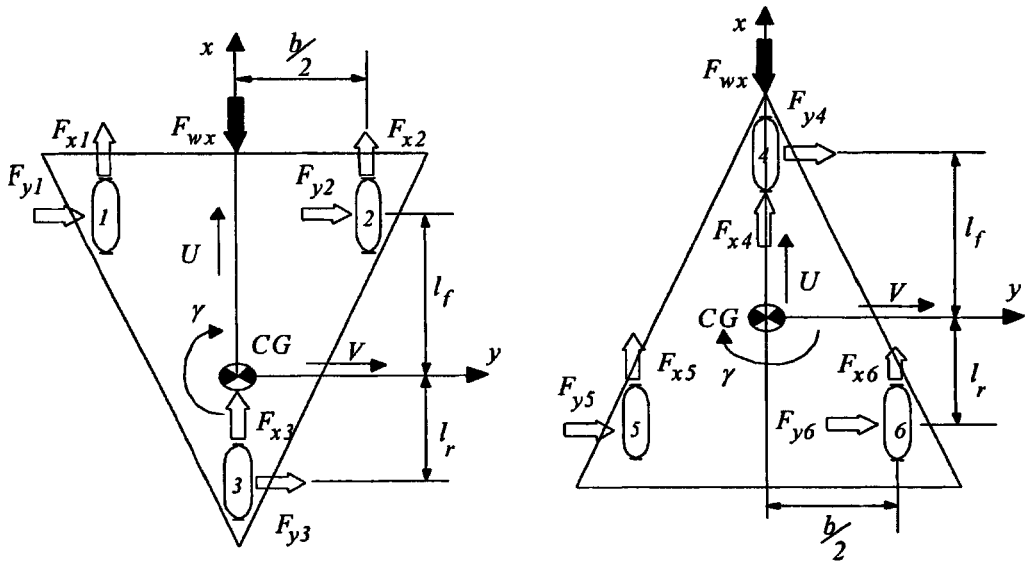

(a) 2F1R three-wheeled vehicle (b) 1F2R three-wheeled vehicle

Fig. 1 Three-wheeled vehicle models

(i.e. the wheels) has only three degrees of freedom, and the body roll, pitch or bounce motions are not allowed. The sprung body, the actual body of vehicle, has the complete six-degree-of-freedom motion. A coordinate frame xyz is fixed to the sprung mass, and the frame $x'y'z'$ is fixed to the unsprung mass. Both origins are at the centre of gravity (CG) of the vehicle. To simplify the model, symmetry exists about the x–z plane of the vehicle.

It is assumed that the sprung mass will revolve about the roll axis and pitch axis of the vehicle. Take the 1F2R three-wheeled vehicle, for example; the roll axis A–A, as shown in Fig. 2b, is the line joining the front and rear roll centres of the vehicle, where the heights of the front and rear roll centres are 0 and h_r. The pitch axis B–B, in Fig. 2b, is the line joining the right and left pitch centres. The vertical distance between the pitch axis and the CG is h_φ. The longitudinal, lateral and yaw motions of the sprung and unsprung bodies are set to be identical.

The velocity of the CG is $\dot{\boldsymbol{R}} = U\boldsymbol{i} + V\boldsymbol{j} + \dot{q}\boldsymbol{k} = U\boldsymbol{i}' + V\boldsymbol{j}' + \dot{q}\boldsymbol{k}'$, where $\boldsymbol{R}$ is the position vector of the CG, and $\boldsymbol{i}, \boldsymbol{j}, \boldsymbol{k}$ and $\boldsymbol{i}', \boldsymbol{j}', \boldsymbol{k}'$ are the unit vectors of the xyz and $x'y'z'$ coordinate systems. The inertia forces and derivatives of angular momentum for the sprung and unsprung mass centres can be obtained as follows:

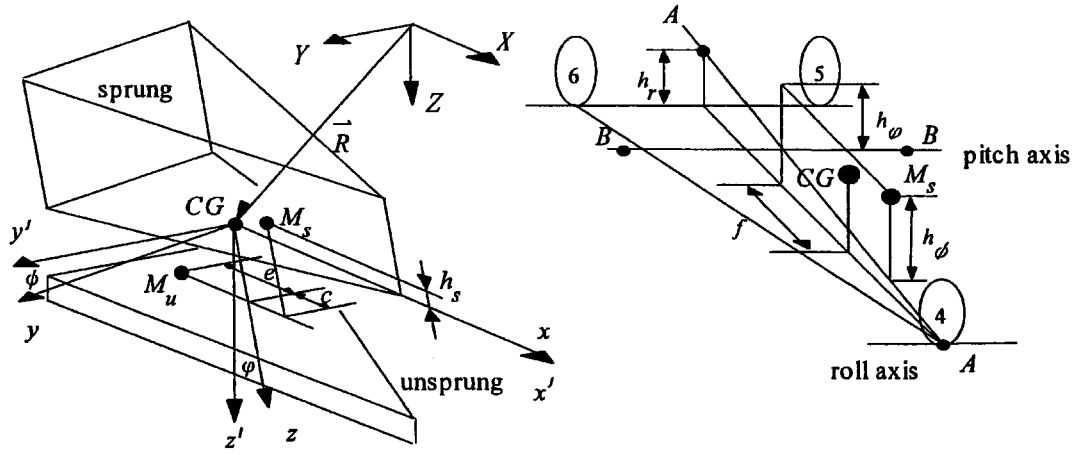

(a) Sprung and unsprung (b) Roll and pitch axes

Fig. 2 Vehicle model with sprung and unsprung bodies

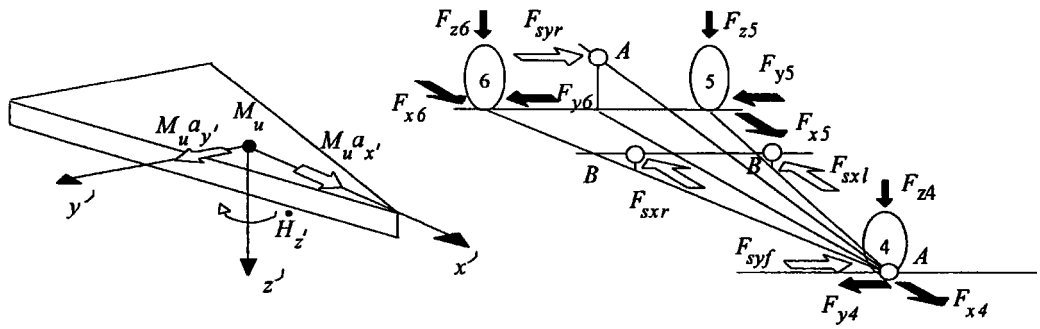

(a) Inertia forces (b) External forces

Fig. 3 Kinetic model of an unsprung mass

$$
\begin{aligned}
M_s a_x &= M_s[\dot{U} - h_s\ddot{\varphi} - \gamma(\dot{V} + h_s\dot{\phi} + c\gamma) + \dot{\varphi}(\dot{q} - c\dot{\varphi})] \\
M_s a_y &= M_s[\dot{V} + h_s\ddot{\phi} + c\dot{\gamma} + \gamma(U - h_s\dot{\varphi}) - \dot{\phi}(\dot{q} - c\dot{\varphi})] \\
M_s a_z &= M_s[(\ddot{q} - c\ddot{\varphi}) - \dot{\varphi}(U - h_s\dot{\varphi}) + \dot{\phi}(V + c\gamma + h_s\dot{\phi})] \\
M_u a_{x'} &= M_u[\dot{U} - \gamma(V - e\gamma)] \\
M_u a_{y'} &= M_u(\dot{V} - e\dot{\gamma} + U\gamma) \\
\dot{H}_x &= I_{xxs}\ddot{\phi} - I_{xzs}\dot{\gamma} - I_{yys}\dot{\varphi}\gamma + \dot{\varphi}(I_{zzs}\gamma - I_{xzs}\dot{\phi}) \\
\dot{H}_y &= I_{yys}\ddot{\varphi} + \gamma(I_{xxs}\dot{\phi} - I_{xzs}\gamma) - \dot{\phi}(I_{zzs}\gamma - I_{xzs}\dot{\phi}) \\
\dot{H}_z &= I_{zzs}\dot{\gamma} - I_{xzs}\ddot{\phi} + I_{yys}\dot{\phi}\dot{\varphi} - \dot{\varphi}(I_{xxs}\dot{\phi} - I_{xzs}\gamma) \\
\dot{H}_{z'} &= I_{zzs}\dot{\gamma}
\end{aligned}
\tag{1}
$$

Since the roll and pitch axes are similar to the hinged joints, only forces, not moments, can be transmitted through them. It is, then, further assumed that the lateral forces will be transmitted from the unsprung to the sprung mass through the roll centres and no roll moment will be induced. The same is true for the pitch motion (i.e. the longitudinal forces will be transmitted through the pitch centres and no pitch moment will be induced). Kinetic analyses for the unsprung mass and sprung mass are carried out individually, and then combined with each other by means of the reaction forces F_{rxl}, F_{rxr}, F_{ryf} and F_{ryr}, which act onto the roll centres and pitch centres, as shown in Figs 3 and 4. After some manipulations, the equations of motion for the 1F2R three-wheeled vehicle are derived as follows:

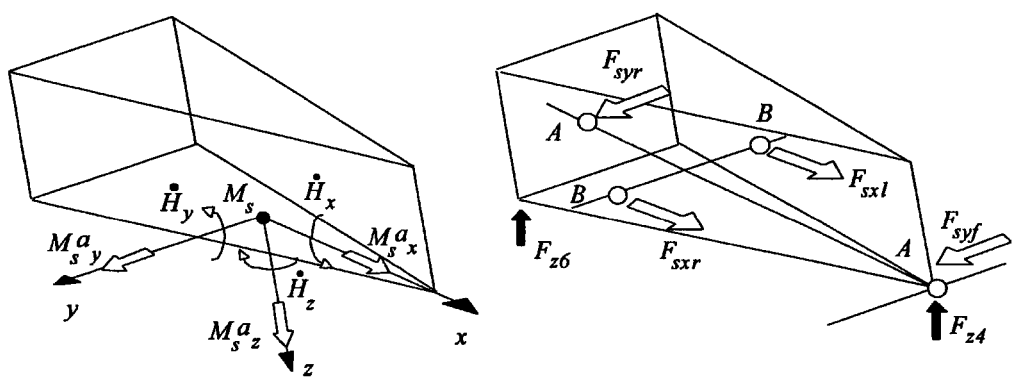

(a) Inertia forces (b) External forces

Fig. 4 Kinetic model of a sprung mass

$$
\begin{aligned}
&M(\dot{U}-V\gamma)-M_{\mathrm{s}}[h_{\mathrm{s}}(\ddot{\varphi}+\dot{\phi}\gamma)-\dot{\varphi}(\dot{q}-c\dot{\varphi})]\\
&\quad=F_{x4}+F_{x5}+F_{x6}-F_{\mathrm{w}x}\\
&M(\dot{V}+U\gamma)+M_{\mathrm{s}}[h_{\mathrm{s}}(\ddot{\phi}-\dot{\varphi}\gamma)-\dot{\phi}(\dot{q}-c\dot{\varphi})]\\
&\quad=F_{y4}+F_{y5}+F_{y6}\\
&I_{\gamma}\dot{\gamma}+I_{z}\dot{\phi}\dot{\varphi}-I_{xz4}(\ddot{\phi}-\dot{\varphi}\gamma)-M_{\mathrm{s}}c\dot{\phi}\dot{q}\\
&\quad=l_{\mathrm{f}}F_{y4}-l_{\mathrm{r}}(F_{y5}+F_{y6})+\frac{b}{2}(F_{x5}-F_{x6})\\
&I_{\phi}\ddot{\phi}+I_{x}\dot{\varphi}\gamma-I_{xz1}(\dot{\gamma}+\dot{\phi}\dot{\varphi})+M_{\mathrm{s}}h_{\phi}\\
&\quad(\dot{V}+U\gamma-\dot{\phi}\dot{q})+M_{\phi,\mathrm{r}}=\frac{b}{2}(F_{z6}-F_{z5})\\
&I_{\varphi}\ddot{\varphi}+I_{y}\dot{\phi}\gamma-I_{xz2}\gamma^{2}+I_{xz3}\dot{\phi}^{2}-M_{\mathrm{s}}h_{\varphi}\\
&\quad[\dot{U}-V\gamma+\dot{\varphi}(\dot{q}-c\dot{\varphi})]-M_{\mathrm{s}}(f+c)\\
&\quad[\ddot{q}-\dot{\varphi}(U-h_{\mathrm{s}}\dot{\varphi})+V\dot{\phi}]+M_{\varphi,\mathrm{r}}\\
&\qquad=(l_{\mathrm{r}}-f)(F_{z5}+F_{z6})-(l_{\mathrm{f}}+f)F_{z4}\\
&M_{\mathrm{s}}[(\ddot{q}-c\ddot{\varphi})-\dot{\varphi}(U-h_{\mathrm{s}}\dot{\varphi})+\dot{\phi}(V+c\gamma+h_{\mathrm{s}}\dot{\phi})]\\
&\quad+F_{q,\mathrm{r}}=F_{z4}+F_{z5}+F_{z6}
\end{aligned}
\tag{2}
$$

where

$$
\begin{aligned}
&I_{\phi}=I_{x\mathrm{s}}+M_{\mathrm{s}}h_{\mathrm{s}}h_{\phi}\\
&I_{\varphi}=I_{y\mathrm{s}}+M_{\mathrm{s}}h_{\mathrm{s}}h_{\varphi}+M_{\mathrm{s}}c(f+c)\\
&I_{\gamma}=I_{z\mathrm{s}}+I_{z\mathrm{u}}+M_{\mathrm{s}}c^{2}+M_{\mathrm{u}}e^{2}\\
&I_{x}=I_{z\mathrm{s}}-I_{y\mathrm{s}}-M_{\mathrm{s}}h_{\mathrm{s}}h_{\phi}\\
&I_{y}=I_{x\mathrm{s}}-I_{z\mathrm{s}}+M_{\mathrm{s}}h_{\mathrm{s}}h_{\varphi}-M_{\mathrm{s}}c(f+c)\\
&I_{z}=I_{y\mathrm{s}}-I_{x\mathrm{s}}+M_{\mathrm{s}}c^{2}\\
&I_{xz1}=I_{xz\mathrm{s}}-M_{\mathrm{s}}h_{\phi}c,\qquad I_{xz2}=I_{xz\mathrm{s}}-M_{\mathrm{s}}h_{\varphi}c\\
&I_{xz3}=I_{xz\mathrm{s}}-M_{\mathrm{s}}h_{\mathrm{s}}(f+c),\qquad I_{xz4}=I_{xz\mathrm{s}}-M_{\mathrm{s}}h_{\mathrm{s}}c\\
&M_{\phi,\mathrm{r}}=\frac{b^{2}}{4}[(C_{\phi5}+C_{\phi6})\dot{\phi}+(K_{\phi5}+K_{\phi6})\phi]\\
&\qquad+\frac{b}{2}[(C_{\phi6}-C_{\phi5})\dot{q}+(K_{\phi6}-K_{\phi5})q]\\
&\qquad+\frac{b}{2}(l_{\mathrm{r}}-f)[(C_{\phi6}-C_{\phi5})\dot{\varphi}+(K_{\phi6}-K_{\phi5})\varphi]\\
&M_{\varphi,r}=(l_{\mathrm{f}}+f)^{2}(C_{\phi4}\dot{\varphi}+K_{\phi4}\varphi)\\
&\qquad+(l_{\mathrm{r}}-f)^{2}[(C_{\phi5}+C_{\phi6})\dot{\varphi}+(K_{\phi5}+K_{\phi6})\varphi]\\
&\qquad-(l_{\mathrm{f}}+f)(C_{\phi4}\dot{q}+K_{\phi4}q)\\
&\qquad+(l_{\mathrm{r}}-f)[(C_{\phi5}+C_{\phi6})\dot{q}+(K_{\phi5}+K_{\phi6})q]\\
&\qquad+\frac{b}{2}(l_{\mathrm{r}}-f)[(C_{\phi6}-C_{\phi5})\dot{\phi}+(K_{\phi6}-K_{\phi5})\phi]\\
&F_{q,\mathrm{r}}=(C_{\phi4}+C_{\phi5}+C_{\phi6})\dot{q}+(K_{\phi4}+K_{\phi5}+K_{\phi6})q\\
&\qquad+(l_{\mathrm{r}}-f)[(C_{\phi5}+C_{\phi6})\dot{\varphi}+(K_{\phi5}+K_{\phi6})\varphi]\\
&\qquad-(l_{\mathrm{f}}+f)(C_{\phi4}\dot{\varphi}+K_{\phi4}\varphi)\\
&\qquad+\frac{b}{2}[(C_{\phi6}-C_{\phi5})\dot{\phi}+(K_{\phi6}-K_{\phi5})\phi]\\
&F_{\mathrm{w}x}=k_{x}U^{2}
\end{aligned}
$$

The linear tyre model is used here for estimating the cornering forces [**8**]. The cornering force F_{yi} acting on the ith tyre is proportional to its slip angle α_i (i.e. $F_{yi}=C_i\alpha_i$, where C_i is the cornering stiffness of the ith tyre). Since the body motion affects the actual steering angle, the ith tyre steer angle should include the tyre roll steer angle θ_i (i.e. $\theta_i=f_i\phi$), where the roll steer coefficient f_i is the rate of change of the ith roll steer angle with respect to the roll angle ϕ [**7**]. If vehicle motion behaviour is $U\gg V$ and $U\gg b\gamma/2$, then the tyre slip angle can be expressed as

$$
\begin{aligned}
\alpha_4&=(\delta_4+\theta_4)-\tan^{-1}\frac{V+l_{\mathrm{f}}\gamma}{U-b\gamma/2}\\
&\approx(\delta_4+\theta_4)-\frac{V+l_{\mathrm{f}}\gamma}{U}\\
\alpha_5&=(\delta_5+\theta_5)-\tan^{-1}\frac{V-l_{\mathrm{r}}\gamma}{U-b\gamma/2}\\
&\approx(\delta_5+\theta_5)-\frac{V-l_{\mathrm{r}}\gamma}{U}\\
\alpha_6&\approx(\delta_6+\theta_6)-\frac{V-l_{\mathrm{r}}\gamma}{U}
\end{aligned}
\tag{3}
$$

If equation (3) is combined with equation (2), the governing equations of the 1F2R three-wheeled vehicle can be formulated in terms of longitudinal velocity U, lateral velocity V, bounce q, roll ϕ, pitch φ and yaw velocity γ, as shown in the following equation:

$$[\mathbf{D}] + \begin{bmatrix} 0 \\ Y_{\phi,\mathrm{r}}\phi + F_{V,\mathrm{r}} \\ N_{\phi,\mathrm{r}}\phi + M_{\gamma,\mathrm{r}} \\ M_{\phi,\mathrm{r}} \\ M_{\varphi,\mathrm{r}} \\ F_{q,\mathrm{r}} \end{bmatrix} = [\mathbf{E}_\mathrm{r}]$$

$$= \begin{bmatrix} 1 \\ 0 \\ 0 \\ 0 \\ 0 \\ 0 \end{bmatrix} F_{x4} + \begin{bmatrix} 1 \\ 0 \\ b/2 \\ 0 \\ 0 \\ 0 \end{bmatrix} F_{x5} + \begin{bmatrix} 1 \\ 0 \\ -b/2 \\ 0 \\ 0 \\ 0 \end{bmatrix} F_{x6} + \begin{bmatrix} 0 \\ C_4 \\ l_\mathrm{f} C_4 \\ 0 \\ 0 \\ 0 \end{bmatrix} \delta_4$$

$$+ \begin{bmatrix} 0 \\ C_\mathrm{r} \\ -l_\mathrm{r} C_\mathrm{r} \\ 0 \\ 0 \\ 0 \end{bmatrix} (\delta_5 + \delta_6) + \begin{bmatrix} 0 \\ 0 \\ 0 \\ 0 \\ -(l_\mathrm{f} + f) \\ 1 \end{bmatrix} F_{z4}$$

$$+ \begin{bmatrix} 0 \\ 0 \\ 0 \\ -b/2 \\ l_\mathrm{r} - f \\ 1 \end{bmatrix} F_{z5} + \begin{bmatrix} 0 \\ 0 \\ 0 \\ b/2 \\ l_\mathrm{r} - f \\ 1 \end{bmatrix} F_{z6} \tag{4}$$

Similarly, the governing equations of the 2F1R three-wheeled vehicle are derived:

$$[\mathbf{D}] + \begin{bmatrix} 0 \\ Y_{\phi,\mathrm{f}}\phi + F_{V,\mathrm{f}} \\ N_{\phi,\mathrm{f}}\phi + M_{\gamma,\mathrm{f}} \\ M_{\phi,\mathrm{f}} \\ M_{\varphi,\mathrm{f}} \\ F_{q,\mathrm{f}} \end{bmatrix} = [\mathbf{E}_\mathrm{f}]$$

$$= \begin{bmatrix} 1 \\ 0 \\ b/2 \\ 0 \\ 0 \\ 0 \end{bmatrix} F_{x1} + \begin{bmatrix} 1 \\ 0 \\ -b/2 \\ 0 \\ 0 \\ 0 \end{bmatrix} F_{x2} + \begin{bmatrix} 1 \\ 0 \\ 0 \\ 0 \\ 0 \\ 0 \end{bmatrix} F_{x3}$$

$$+ \begin{bmatrix} 0 \\ C_\mathrm{f} \\ l_\mathrm{f} C_\mathrm{f} \\ 0 \\ 0 \\ 0 \end{bmatrix} (\delta_1 + \delta_2) + \begin{bmatrix} 0 \\ C_3 \\ -l_\mathrm{r} C_3 \\ 0 \\ 0 \\ 0 \end{bmatrix} \delta_3 + \begin{bmatrix} 0 \\ 0 \\ 0 \\ -b/2 \\ -(l_\mathrm{f} + f) \\ 1 \end{bmatrix} F_{z1}$$

$$+ \begin{bmatrix} 0 \\ 0 \\ 0 \\ b/2 \\ -(l_\mathrm{f} + f) \\ 1 \end{bmatrix} F_{z2} + \begin{bmatrix} 0 \\ 0 \\ 0 \\ 0 \\ l_\mathrm{r} - f \\ 1 \end{bmatrix} F_{z3} \tag{5}$$

where $[\mathbf{E}_\mathrm{f}]$ and $[\mathbf{E}_\mathrm{r}]$ are both 6×1 matrices and $[\mathbf{D}] = [d_1\ d_2\ d_3\ d_4\ d_5\ d_6]^\mathrm{T}$:

$$d_1 = M(\dot{U} - V\gamma) - M_\mathrm{s}[h_\mathrm{s}(\ddot{\varphi} + \dot{\phi}\gamma) - \dot{\varphi}(\dot{q} - c\dot{\varphi})] + K_x U^2$$

$$d_2 = M(\dot{V} + U\gamma) + M_\mathrm{s}[h_\mathrm{s}(\ddot{\phi} - \dot{\varphi}\gamma) - \dot{\phi}(\dot{q} - c\dot{\varphi})]$$

$$d_3 = I_\gamma\dot{\gamma} + I_z\dot{\phi}\dot{\varphi} - I_{xz4}(\ddot{\phi} - \dot{\varphi}\gamma) - M_\mathrm{s}c\dot{\phi}\dot{q}$$

$$d_4 = I_\phi\ddot{\phi} + I_x\dot{\varphi}\gamma - I_{xz1}(\dot{\gamma} + \dot{\phi}\dot{\varphi}) + M_\mathrm{s}h_\phi(\dot{V} + U\gamma - \dot{\phi}\dot{q})$$

$$d_5 = I_\varphi\ddot{\varphi} + I_y\dot{\phi}\gamma - I_{xz2}\gamma^2 + I_{xz3}\dot{\phi}^2 - M_\mathrm{s}h_\varphi[\dot{U} - V\gamma + \dot{\varphi}(\dot{q} - c\dot{\varphi})] - M_\mathrm{s}(f + c)[\ddot{q} - \dot{\varphi}(U - h_\mathrm{s}\dot{\varphi}) + V\dot{\phi}]$$

$$d_6 = M_s[(\ddot{q} - c\ddot{\varphi}) - \dot{\varphi}(U - h_s\dot{\varphi}) + \dot{\phi}(V + c\gamma + h_s\dot{\phi})]$$

$$Y_{\phi,r} = -C_4 f_4 - C_r(f_5 + f_6)$$

$$F_{V,r} = \frac{1}{U}[V(C_4 + 2C_r) + \gamma(l_f C_4 - 2l_r C_r)]$$

$$N_{\phi,r} = -l_f C_4 f_4 + l_r C_r(f_5 + f_6)$$

$$M_{\gamma,r} = \frac{1}{U}[V(l_f C_4 - 2l_r C_r) + \gamma(l_f^2 C_4 + 2l_r^2 C_r)]$$

$$Y_{\phi,f} = -C_f(f_1 + f_2) - C_3 f_3$$

$$F_{V,f} = \frac{1}{U}[V(2C_f + C_3) + \gamma(2l_f C_f - l_r C_3)]$$

$$N_{\phi,f} = -l_f C_f(f_1 + f_2) + l_r C_3 f_3$$

$$M_{\gamma,f} = \frac{1}{U}[V(2l_f C_f - l_r C_3) + \gamma(2l_f^2 C_f + l_r^2 C_3)]$$

$$M_{\phi,f} = \frac{b^2}{4}[(C_{\phi 1} + C_{\phi 2})\dot{\phi} + (K_{\phi 1} + K_{\phi 2})\phi] + \frac{b}{2}[(C_{\phi 2} - C_{\phi 1})\dot{q} + (K_{\phi 2} - K_{\phi 1})q] + \frac{b}{2}(l_f + f)[(C_{\phi 1} - C_{\phi 2})\dot{\varphi} + (K_{\phi 1} - K_{\phi 2})\varphi]$$

$$M_{\varphi,f} = (l_f + f)^2[(C_{\phi 1} + C_{\phi 2})\dot{\varphi} + (K_{\phi 1} + K_{\phi 2})\varphi] + (l_r - f)^2(C_{\phi 3}\dot{\varphi} + K_{\phi 3}\varphi) - (l_f + f)[(C_{\phi 1} + C_{\phi 2})\dot{q} + (K_{\phi 1} + K_{\phi 2})q] + (l_r - f)(C_{\phi 3}\dot{q} + K_{\phi 3}q) + \frac{b}{2}(l_f + f)[(C_{\phi 1} - C_{\phi 2})\dot{\phi} + (K_{\phi 1} - K_{\phi 2})\phi]$$

$$F_{q,f} = (C_{\phi 1} + C_{\phi 2} + C_{\phi 3})\dot{q} + (K_{\phi 1} + K_{\phi 2} + K_{\phi 3})q + (l_r - f)(C_{\phi 3}\dot{\varphi} + K_{\phi 3}\varphi) - (l_f + f)[(C_{\phi 1} + C_{\phi 2})\dot{\varphi} + (K_{\phi 1} + K_{\phi 2})\varphi] + \frac{b}{2}[(C_{\phi 2} - C_{\phi 1})\dot{\phi} + (K_{\phi 2} - K_{\phi 1})\phi]$$

From equations (4) and (5), the tractive forces on the same side, or the steering angles of the wheels on the same axle will have the same effects on the motion. Therefore, these parameters can be combined, and let

$$F_{xl} = F_{x1} = F_{x5}, \qquad F_{xr} = F_{x2} = F_{x6}$$

$$\delta_f = \delta_1 + \delta_2 = \delta_4, \qquad \delta_r = \delta_3 = \delta_5 + \delta_6$$

$$F_{zl} = F_{zl} = F_{z5}, \qquad F_{zr} = F_{z2} = F_{z6}$$

$$F_{zl} = F_{z3} = F_{z4}$$

The final eight control parameters are the left-side, right-side and singled-wheel tractive forces, front and rear steering angles, and three active suspension forces (i.e. F_{xl}, F_{xr}, F_{xs}, δ_f, δ_r, F_{zl}, F_{zr}, F_{zs}).

3 FULL CONTROL MODES

As the vehicle has a zero body sideslip angle, the lateral velocity and acceleration must diminish; $\dot{V} = V = 0$. For the zero body motions, the pitch, roll and bounce motions of the vehicle are not allowed, and $\dot{\phi} = \phi = \dot{\varphi} = \varphi = \dot{q} = q = 0$. After substitution of these values into equations (4) and (5), it follows that

$$[\mathbf{E}_f] = \begin{bmatrix} M\dot{U} + K_x U^2 \\ MU\gamma + \dfrac{(2l_f C_f - l_r C_3)\gamma}{U} \\ I_\gamma\dot{\gamma} + \dfrac{(2l_f^2 C_f + l_r^2 C_3)\gamma}{U} \\ -I_{xzl}\dot{\gamma} + M_s h_\phi U\gamma \\ -I_{xz2}\gamma^2 - M_s h_\varphi \dot{U} \\ 0 \end{bmatrix}$$

$$[\mathbf{E}_r] = \begin{bmatrix} M\dot{U} + K_x U^2 \\ MU\gamma + \dfrac{(l_f C_4 - 2l_r C_r)\gamma}{U} \\ I_\gamma\dot{\gamma} + \dfrac{(l_f^2 C_4 + 2l_r^2 C_r)\gamma}{U} \\ -I_{xz1}\dot{\gamma} + M_s h_\phi U\gamma \\ -I_{xz2}\gamma^2 - M_s h_\varphi \dot{U} \\ 0 \end{bmatrix} \tag{6}$$

Here it should be assumed that the prescribed driving scenarios of the two three-wheeled vehicles are the same in order to compare their relative performance (i.e. $C_4 = 2C_f$ and $C_6 = 2C_r$). This means that the cornering force produced from the singled wheel of one three-wheeled vehicle is the same as that produced from the

Table 1 Expressions for [**G**]

Q1: F_{xl}, F_{xr}, δ_f	Q2: F_{xl}, F_{xs}, δ_f	Q3: F_{xr}, F_{xs}, δ_f	Q4: F_{xl}, F_{xr}, δ_r	Q5: F_{xl}, F_{xs}, δ_r
$\begin{bmatrix} 1 & 1 & 0 \\ 0 & 0 & C_f \\ b/2 & -b/2 & l_f C_f \end{bmatrix}$	$\begin{bmatrix} 1 & 1 & 0 \\ 0 & 0 & C_f \\ b/2 & 0 & l_f C_f \end{bmatrix}$	$\begin{bmatrix} 1 & 1 & 0 \\ 0 & 0 & C_f \\ -b/2 & 0 & l_f C_f \end{bmatrix}$	$\begin{bmatrix} 1 & 1 & 0 \\ 0 & 0 & C_r \\ b/2 & -b/2 & -l_r C_r \end{bmatrix}$	$\begin{bmatrix} 1 & 1 & 0 \\ 0 & 0 & C_r \\ b/2 & 0 & -l_r C_r \end{bmatrix}$

Q6: F_{xr}, F_{xs}, δ_r	Q7: F_{xl}, δ_f, δ_r	Q8: F_{xr}, δ_f, δ_r	Q9: F_{xs}, δ_f, δ_r
$\begin{bmatrix} 1 & 1 & 0 \\ 0 & 0 & C_r \\ -b/2 & 0 & -l_r C_r \end{bmatrix}$	$\begin{bmatrix} 1 & 0 & 0 \\ 0 & C_f & C_r \\ b/2 & l_f C_f & -l_r C_r \end{bmatrix}$	$\begin{bmatrix} 1 & 0 & 0 \\ 0 & C_f & C_r \\ -b/2 & l_f C_f & -l_r C_r \end{bmatrix}$	$\begin{bmatrix} 1 & 0 & 0 \\ 0 & C_f & C_r \\ 0 & l_f C_f & -l_r C_r \end{bmatrix}$

two side wheels of the other three-wheeled vehicle. Then

$$[\mathbf{E}] = [\mathbf{E}_f] = [\mathbf{E}_r] = \begin{bmatrix} M\dot{U} + K_x U^2 \\ MU\gamma + \dfrac{2(l_f C_f - l_r C_r)\gamma}{U} \\ I_\gamma \dot{\gamma} + \dfrac{2(l_f^2 C_f + l_r^2 C_r)\gamma}{U} \\ -I_{xz1}\dot{\gamma} + M_s h_\phi U \gamma \\ -I_{xz2}\gamma^2 - M_s h_\phi \dot{U} \\ 0 \end{bmatrix} \tag{7}$$

Full control means that the motion of a vehicle can be controlled fully, such that a prescribed driving scenario can be achieved. Among these eight control parameters, only six should be selected and controlled. Let n_1, n_2, n_3, n_4, n_5 and n_6 be the chosen six full control parameters and arrange equations (4) and (5) in matrix form, as shown below:

$$[\mathbf{E}] = [\mathbf{F}][n_1\ n_2\ n_3\ n_4\ n_5\ n_6]^T$$
$$[n_1\ n_2\ n_3\ n_4\ n_5\ n_6]^T = [\mathbf{F}]^{-1}[\mathbf{E}] \tag{8}$$

Here [**F**] is a 6×6 influence coefficient matrix, formed by combining the corresponding coefficients of the chosen six control parameters.

From equations (4) and (5), the vehicle longitudinal, lateral and yaw motions are only related to the tractive forces and steering angles, and the body motions are only related to the active suspension forces. Therefore, the control parameters can be separated into two groups. [**F**] can also be separated into two submatrices: matrix [**G**], related to the tractive forces and steering angles, and matrix [**H**], which is related to the active suspension forces.

For these control inputs to have physical meanings, it is necessary that $[\mathbf{F}]^{-1}$ must exist, i.e. det $[\mathbf{F}] \neq 0$. This implies that both det $[\mathbf{G}] \neq 0$ and det $[\mathbf{H}] \neq 0$, and [**G**] and [**H**] must be 3×3 positive definite matrices:

$$[\mathbf{F}]_{6\times6} = \begin{bmatrix} [\mathbf{G}]_{3\times3} & [\mathbf{0}]_{3\times3} \\ [\mathbf{0}]_{3\times3} & [\mathbf{H}]_{3\times3} \end{bmatrix}$$
$$\det[\mathbf{F}] = \det[\mathbf{G}] \det[\mathbf{H}] \neq 0 \tag{9}$$

Among the five tractive forces and steering angles, only and at most three could be selected. Nine control modes, Q1 to Q9, for the traction and steering can be formulated and [**G**] can be found, as shown in Table 1. In modes Q1 to Q6, only one single steering angle is selected as an input. In modes Q1 to Q3, the steering is in the front wheels, and in modes Q4 to Q6, in the rear. In modes Q7 to Q9, both the front and the rear wheels can be steered, but only one wheel has the tractive force.

Three active suspension forces can be applied in each of the three-wheeled vehicles. Two different control modes, 2F1R and 1F2R, and the corresponding [**H**] can be found, as shown in Table 2.

By means of commutative combination of tractive forces, steering angles and active suspension forces in three-wheeled vehicles, there are a total of nine control modes. It can be easily checked that the determinant of [**G**] and [**H**] should not be zero. This will ensure that control inputs are solvable and the system can be controlled.

4 EVALUATION CRITERIA FOR FULL CONTROL MODES

Any one of the nine full control modes will allow the

Table 2 Expressions for [**H**]

2F1R: F_{zl}, F_{zr}, F_{zx}	1F2R: F_{zs}, F_{zl}, F_{zr}
$\begin{bmatrix} -b/2 & b/2 & 0 \\ -(l_f + f) & -(l_f + f) & l_r - f \\ 1 & 1 & 1 \end{bmatrix}$	$\begin{bmatrix} 0 & -b/2 & b/2 \\ -(l_f + f) & l_r - f & l_r - f \\ 1 & 1 & 1 \end{bmatrix}$

vehicle to follow a determined motion scenario. Here, the performance of these modes will not be compared by means of a traditional steady state, time or frequence response. In order to compare the selection of control parameters and control modes, three evaluation criteria are proposed: (a) the sum of tractive forces, (b) the sum of cornering forces and (c) the sum of active suspension forces. These three evaluating forces have significant practical meanings. They are outlined and explained as follows.

4.1 Sum of tractive forces F_{xt}

The sum of needed tractive forces is a useful index to show the effectiveness of the use of energy. Larger tractive forces should be avoided. This can be shown as

$$F_{xt} = \frac{F_{xl} + |F_{xl}|}{2} + \frac{F_{xr} + |F_{xr}|}{2} \tag{10}$$

When the tractive force has a negative value, the wheel is braking. Since the braking will not demand energy from the power plant, it will be ignored here. In equation (10), the negative tractive force will be cancelled. However, it is worthwhile to point out that, if energy can be retrieved, such as from electric brakes, the negative tractive forces can be favoured.

4.2 Sum of cornering forces F_{yt}

The cornering force would result in excessive tyre wear and fatigue due to the heat build-up. A lower cornering force is more favourable. The sum of needed cornering forces is expressed as

$$\begin{aligned} F_{yt} &= |F_{y1} + F_{y2}| + |F_{y3} + F_{y4}| \\ &= \left|C_f\left(\delta_f - 2\frac{V + l_f\gamma}{U}\right)\right| + \left|C_r\left(\delta_r - 2\frac{V - l_r\gamma}{U}\right)\right| \end{aligned} \tag{11}$$

4.3 Sum of active suspension forces F_{zt}

The active suspension forces are generated by the actuators, and the sum of needed active suspension forces directly represents the energy consumption of the actuators. A lower active suspension force means less energy transmitted into the system, and it will be favoured. The sum of needed active suspension forces is expressed as

$$F_{zt} = \sum_{i=1}^{4} |F_{zi}| \tag{12}$$

The control mode that needs less overall tractive force, cornering force and active suspension force will be more energy efficient and produce less scuff power loss. The comparison of full control modes will be based on these three evaluated forces.

5 COMPARISON OF FULL CONTROL MODES

Two driving scenarios are discussed here for comparison of the difference between the control modes. The first is a vehicle straight-line run, and the second is a vehicle negotiating a constant radius turn.

5.1 Straight-line run

The straight-line run is a rather simple case of vehicle control. The discussion here shows that choosing different sets of control inputs leads to very different results. The vehicle yaw velocity is set be zero, and the corresponding inverse matrix $[\mathbf{F}]^{-1}$ of each control mode is obtained. If they are substituted into equation (8), expressions for the control parameters are found, as shown in Table 3. These are then substituted into equations (10) to (12) to find the evaluating forces (the sum of the tractive forces, cornering force, and active suspension forces in each modes), shown in Table 4, where $\delta = \delta_f$ in modes Q1, Q2 and Q3 and $\delta = \delta_r$ in modes Q4, Q5 and Q6.

Vehicles with a constant speed and with acceleration are both discussed here.

5.1.1 Straight-line run with a constant speed

With no accelerations, $\dot{U} = 0$, as shown in Table 3, all

Table 3 Expressions for control parameters in the straight-line run

Q1, Q4	$F_{xl} = \frac{1}{2}P_1$, $F_{xr} = \frac{1}{2}P_1$, $\delta = 0$	Q2, Q5	$F_{xl} = 0$, $F_{xs} = P_1$, $\delta = 0$
Q3, Q6	$F_{xr} = 0$, $F_{xs} = P_1$, $\delta = 0$	Q7	$F_{xl} = P_1, \delta_f = -\frac{b}{2lC_f}P_1, \delta_r = \frac{b}{2lC_r}P_1$
Q8	$F_{xr} = P_1, \delta_f = \frac{b}{2lC_f}P_1, \delta_r = -\frac{b}{2lC_r}P_1$	Q9	$F_{xs} = P_1$, $\delta_f = 0$, $\delta_r = 0$
2F1R	$F_{zl} = F_{zr} = \frac{M_s h_\varphi \dot{U}}{2l}$, $F_{zs} = -\frac{M_s h_\varphi \dot{U}}{l}$	1F2R	$F_{zs} = \frac{M_s h_\varphi \dot{U}}{l}$, $F_{zl} = F_{zr} = -\frac{M_s h_\varphi \dot{U}}{2l}$

$P_1 = M\dot{U} + k_x U^2$.

Table 4 Expressions for evaluating forces in the straight-line run

	F_{xt}	F_{yt}		F_{zt}
Q1 to Q6, Q9	P_1	0	2F1R	$\frac{2M_s h_\varphi \dot{U}}{l}$
Q7, Q8	P_1	$\frac{bP_1}{l}$	1F2R	$\frac{2M_s h_\varphi \dot{U}}{l}$

three active suspension forces are zero. However, the selection of the steering angles and tractive forces does make a difference. In modes Q1 to Q6 there is only one steering angle input, and it is always zero. Two tractive forces on the two sides in modes Q1 and Q4 are equal. Only the singled wheel provides a tractive force in modes Q2 and Q3 and modes Q5 and Q6, and the aside tractive force is always zero.

In modes Q7 and Q8, there is only a tractive force on an aside wheel of the vehicle. The side tractive force results in a yaw moment, and this must be balanced by the cornering forces provided by the two sets of steering wheels. Take mode Q7, for example: the tractive force is on the left side, and the front wheels must turn to the left and the rear to the right. It is rather unusual that, in the straight-line run, steering angles are not zero, and the excessive cornering forces is certainly not desirable.

In mode Q9, because the only tractive force provided by the singled wheel will not result in a yaw moment, two steering angle inputs are always zero.

5.1.2 *Straight-line run with an acceleration*

The needed tractive forces and steering angles increase, because $\dot{U}$ is no longer zero. Furthermore, because of acceleration, proper active suspension forces must be applied in order to maintain the zero body motions. The active suspension forces, exerted on the front and rear axles are equal in magnitude, opposite in direction and equal on both sides, as shown in Table 3.

5.1.3 *Current remarks*

When a vehicle undertakes a straight-line run, all nine full control modes introduce the same total tractive force and total active suspension force. All of the three active suspension forces are useful, and the two sides are always equal. As to the cornering forces, in modes Q7 and Q8, excessive cornering forces appear, but no cornering forces exist in modes Q1 to Q6 and Q9.

For the full control modes, it is possible to choose two tractive forces and only one steering angle as control parameters, such as for modes Q1 to Q6, or to choose two steering angles and the tractive force provided by the singled wheel as control parameters, such as in mode Q9, for the straight-line run. For active suspension force, the three-wheeled vehicles 2F1R and 1F2R exhibit no difference in the straight-line run.

5.2 Constant radius turn

When a vehicle negotiates a constant radius turn, the yaw velocity is U/ρ and yaw acceleration is $\dot{U}/\rho$. As for the previous derivation in the case of the straight-line run, expressions for the control parameters, shown in Table 5, and expressions for the evaluating forces, shown in Table 6, can be found.

Because these expressions are highly complicated, and cannot be analysed by simple means, a numerical approach is used and the numerical simulation results are presented here. The numerical results only provide an estimate of the dynamics of a typical vehicle; they cannot represent all types of vehicles by any means.

A computer program, prepared in MATHEMATICA, is used for finding the numerical values of the control parameters and the evaluating forces. The mass and dimensions of the simulated vehicle are taken from a typical vehicle as listed in Table 7. The vehicle with a constant speed and with an acceleration are both discussed here.

5.2.1 *Constant radius turn with a constant speed*

Using the expressions in Tables 6 and 7, the numerical results of simulation for the control parameters of each control mode are shown in Fig. 5 and the evaluating forces of each control modes are shown in Fig. 6, where 'S', 'L' and 'R' in parentheses represent the singled, left and right wheels respectively of the three-wheeled vehicle.

From Fig. 5, the control modes using only one steering angle, modes Q1 to Q6, demand higher tractive forces and greater steering angles during the turn. In modes Q4 to Q6, the highest tractive forces and the greatest steering angles have been observed. The reason can be that in modes Q4 to Q6 the unsteered front wheel(s) introduces a negative cornering force, and in order to keep from lateral zero force, the rear wheel(s) will need a greater steering angle, and a larger tractive force is then needed to balance the increased negative yaw moment. Therefore, the tractive forces, the steering angles and also the evaluating forces of modes Q4 to Q6 are greater than those for modes Q1 to Q3, as shown in Figs 5 and 6.

Two tractive forces in modes Q1 to Q3, which choose a front steering angle as a control parameter, change their application direction in order to balance the varying yaw moment, which does not change in the cases of modes Q4 to Q6, as shown in Fig. 5a. The control modes using only one steering angle and one tractive force provided by the singled wheel as a control parameter, modes Q2, Q3, Q5 and Q6, demand greater tractive forces than those for modes Q1 and Q4. Because the distance between the two

Table 5 Expressions for control parameters in a constant radius turn

Q1	Q2	Q3	Q4	Q5	Q6
$F_{xl} = \dfrac{P_1 + P_3}{2}$	$F_{xl} = P_3$	$F_{xr} = -P_3$	$F_{xl} = \dfrac{P_1 + P_4}{2}$	$F_{xl} = P_4$	$F_{xr} = -P_4$
$F_{xr} = \dfrac{P_1 - P_3}{2}$	$F_{xs} = P_1 - P_3$	$F_{xs} = P_1 + P_3$	$F_{xr} = \dfrac{P_1 - P_4}{2}$	$F_{xs} = P_1 - P_4$	$F_{xs} = P_1 + P_4$
$\delta_f = \dfrac{P_2}{C_f}$	$\delta_f = \dfrac{P_2}{C_f}$	$\delta_f = \dfrac{P_2}{C_f}$	$\delta_r = \dfrac{P_2}{C_r}$	$\delta_r = \dfrac{P_2}{C_r}$	$\delta_r = \dfrac{P_2}{C_r}$

Q7	Q8	Q9	2F1R	1F2R
$F_{xl} = P_1$	$F_{xr} = P_1$	$F_{xs} = P_1$	$F_{zl} = -P_5 + \dfrac{P_6}{2}$	$F_{zs} = P_6$
$\delta_f = -\dfrac{b(P_1 - P_4)}{2lC_f}$	$\delta_f = \dfrac{b(P_1 + P_4)}{2lC_f}$	$\delta_f = \dfrac{bP_4}{2lC_f}$	$F_{zr} = P_5 + \dfrac{P_6}{2}$	$F_{zl} = -P_5 - \dfrac{P_6}{2}$
$\delta_r = \dfrac{b(P_1 - P_3)}{2lC_r}$	$\delta_r = -\dfrac{b(P_1 + P_3)}{2lC_r}$	$\delta_r = -\dfrac{bP_3}{2lC_r}$	$F_{zs} = -P_6$	$F_{zr} = P_5 - \dfrac{P_6}{2}$

$$P_2 = \frac{2(l_f C_f - l_r C_r) + MU^2}{\rho}$$

$$P_3 = \frac{2}{\rho b}[I_\gamma \dot{U} + (2ll_r C_r - Ml_f U^2)],\ P_4 = \frac{2}{\rho b}[I_\gamma \dot{U} + (2ll_f C_f + Ml_r U^2)]$$

$$P_5 = \frac{1}{\rho b}(M_s h_\phi U^2 - I_{xz1}\dot{U}),\ P_6 = \frac{1}{\rho^2 l}(M_s h_\phi \rho^2 \dot{U} + I_{xz2} U^2)$$

Table 6 Expressions for evaluating forces in a constant radius turn

	F_{xl}		F_{yl}		F_{zl}
Q1	$\dfrac{2P_1 + \lvert P_1 + P_3\rvert + \lvert P_1 - P_3\rvert}{4}$	Q1 to Q3	$\left\lvert P_2 - \dfrac{2l_f C_f}{\rho}\right\rvert + \dfrac{2l_r C_r}{\rho}$	2F1R, 1F2R	$\left\lvert P_5 - \dfrac{P_6}{2}\right\rvert + \left\lvert P_5 + \dfrac{P_6}{2}\right\rvert + \lvert P_6\rvert$
Q2	$\dfrac{P_1 + \lvert P_3\rvert + \lvert P_1 - P_3\rvert}{2}$	Q4 to Q6	$\left\lvert P_2 + \dfrac{2l_r C_r}{\rho}\right\rvert + \dfrac{2l_f C_f}{\rho}$		
Q3	$\dfrac{P_1 + \lvert P_3\rvert + \lvert P_1 + P_3\rvert}{2}$	Q7	$\left\lvert \dfrac{b(P_1 - P_4)}{2l} + \dfrac{2l_f C_f}{\rho}\right\rvert + \left\lvert \dfrac{b(P_1 - P_3)}{2l} + \dfrac{2l_r C_r}{\rho}\right\rvert$		
Q4	$\dfrac{2P_1 + \lvert P_1 + P_4\rvert + \lvert P_1 - P_4\rvert}{4}$	Q8	$\left\lvert \dfrac{b(P_1 - P_4)}{2l} - \dfrac{2l_f C_f}{\rho}\right\rvert + \left\lvert \dfrac{b(P_1 - P_3)}{2l} - \dfrac{2l_r C_r}{\rho}\right\rvert$		
Q5	$\dfrac{P_1 + \lvert P_4\rvert + \lvert P_1 - P_4\rvert}{2}$	Q9	$\left\lvert \dfrac{bP_4}{2l} - \dfrac{2l_f C_f}{\rho}\right\rvert + \left\lvert \dfrac{bP_3}{2l} - \dfrac{2l_r C_r}{\rho}\right\rvert$		
Q6	$\dfrac{P_1 + \lvert P_4\rvert + \lvert P_1 + P_4\rvert}{2}$				
Q7 to Q9	$\dfrac{P_1 + \lvert P_1\rvert}{2}$				

Table 7 Data for the simulated vehicle

$M = 2000$ kg	$C_f = 41\,580$ N/rad	$l = 2.80$ m	$b = 1.48$ m	$h_\phi = 0.25$ m	$\rho = 50$ m
$M_s = 1800$ kg	$C_r = 34\,020$ N/rad	$l_f = 1.26$ m	$c = 0.03$ m	$h_\varphi = 0.3$ m	$U = 0.3$g
$M_u = 200$ kg	$k_x = 0.40$ N s^2/m^2	$l_r = 1.54$ m	$e = 0.27$ m		

wheels in modes Q2, Q3, Q5 and Q6 is smaller, the yaw moment can be balanced only by increasing the tractive forces. Therefore, the total tractive force for modes Q2 and Q3 is greater than that for mode Q1, and correspondingly tractive forces for modes Q5 and Q6 are greater than that for mode Q4, as shown in Fig. 6a.

The cornering force of front and rear wheels will balance the yaw moment generated by the centrifugal

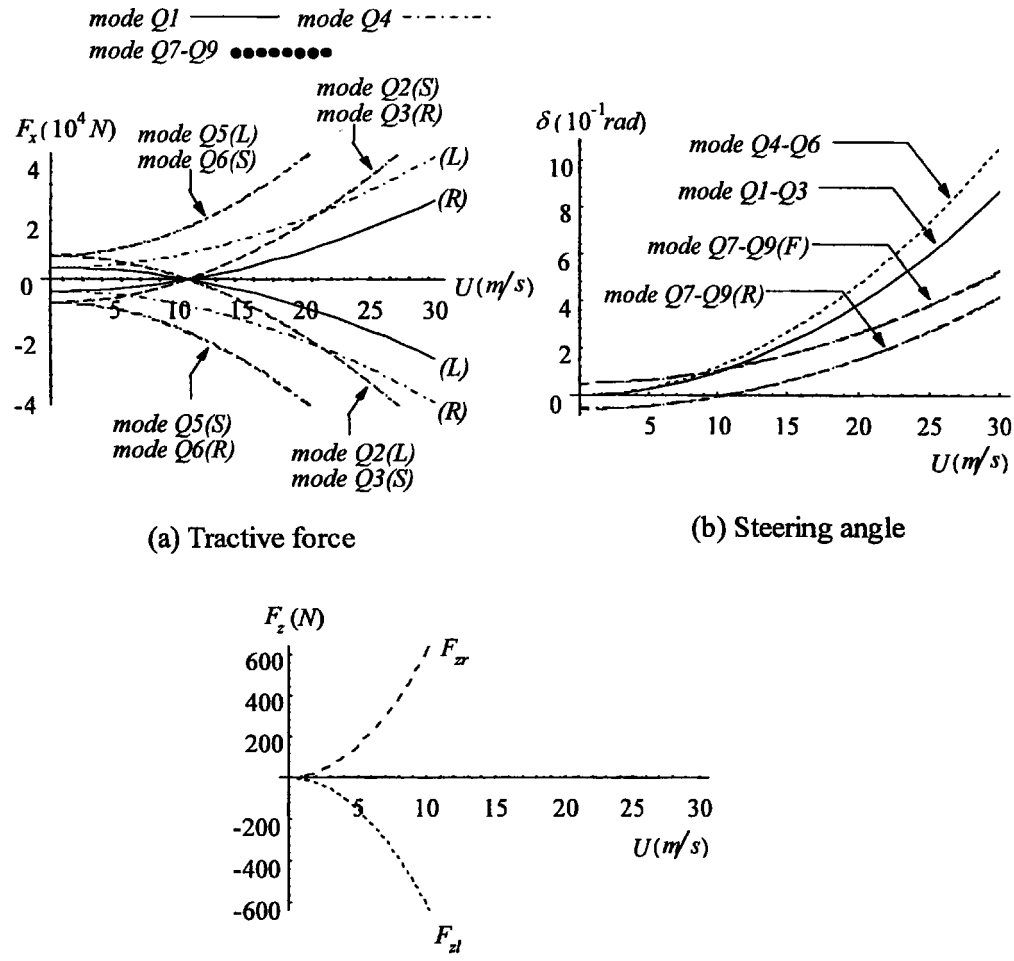

Fig. 5 Control parameters in a constant radius turn with a constant speed

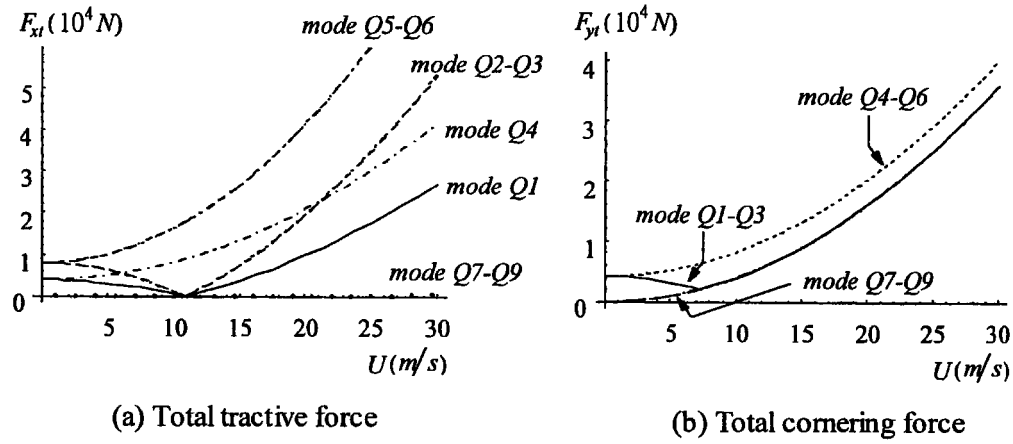

Fig. 6 Evaluating forces in a constant radius turn with a constant speed

force and tractive force in modes Q7 to Q9. With a proper match between the front steering angle and the rear steering angle, the total tractive and cornering forces are less than those for a single steering angle, as shown in Fig. 6.

As to the active suspension forces, two side active suspension forces prevent the vehicle from rolling, as shown in Fig. 5c. The total active suspension force of the three-wheeled vehicles 2F1R and 1F2R are the same.

5.2.2 *Constant radius turn with an acceleration*

Acceleration introduces the longitudinal weight transfer, in addition to the lateral weight transfer caused by the centrifugal force. The results of numerical simulation are shown in Figs 7 and 8.

It is obvious that, with an acceleration, the needed tractive forces should be increased in all the control modes. Because of the increased tractive force, mainly provided by the singled wheel in modes Q2, Q3, Q5 and Q6, the different tractive force between the singled wheel of one mode and the side wheel of the other mode in modes Q2 and Q3 is increased, and it is the same in modes Q5 and Q6 from comparison of Figs 7a and 5a.

The differences between the front steering angle and rear steering angle in mode Q7 are reduced, yet for mode Q8 are increased, from comparison of Figs 7b and 5b. The reason is that, in mode Q7, the increased tractive force on the outside wheel produces a greater yaw moment, helping the vehicle to turn; thus the difference of the front and rear steering angles, which also produces the needed positive yaw moment, can then be reduced. The reverse is true for the mode Q8.

Among the three active suspension forces, the singled wheel either on the front or on the rear axle remains about the same. One of the two active suspension forces paired on an axle changes its direction, such as F_{zl} for the 2F1R vehicle and F_{zr} for the 1F2R vehicle, as shown in Figs 7c and 7d. This phenomenon, that active suspension force

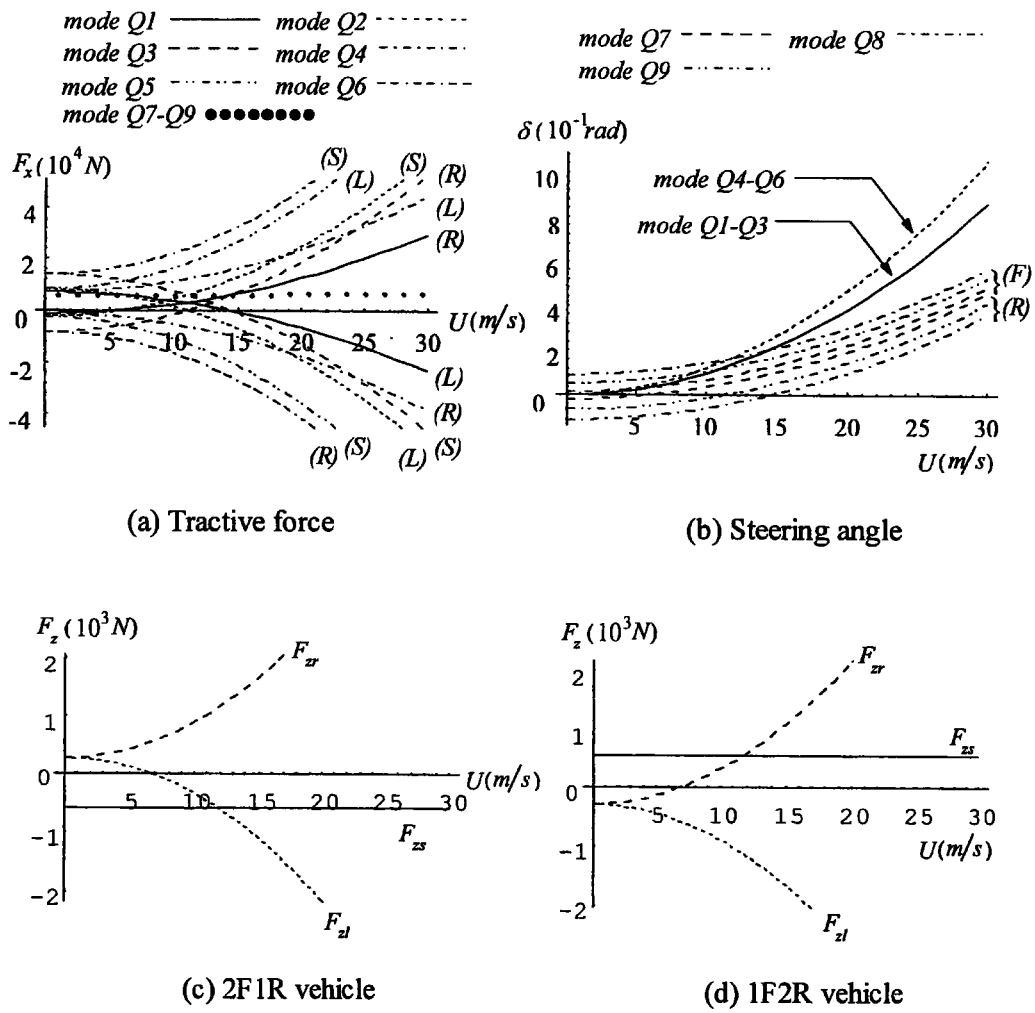

Fig. 7 Control parameters in a constant radius turn with an acceleration

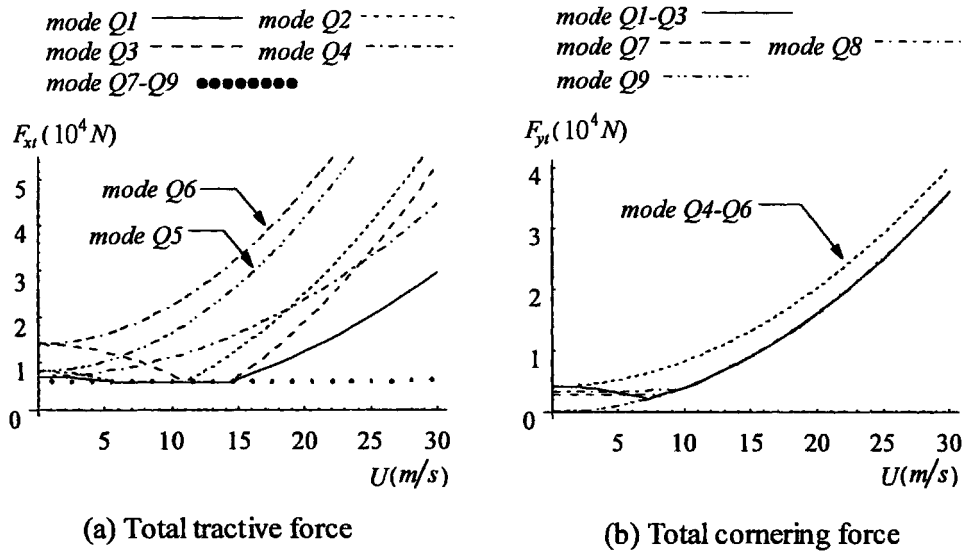

Fig. 8 Evaluating forces in a constant radius turn with an acceleration

changes the direction of its application, is, as the result of taking the dynamic weight transfer, caused by both the intertia and centrifugal force.

As in the case with a constant speed, the control modes using only one steering angle, modes Q1 to Q6, demand a greater total tractive force during the turn than in the modes Q7 to Q9. The total cornering forces of modes Q7, Q8 and Q1 to Q3 are about the same. In modes Q4 to Q6, the highest total tractive force is for the mode Q6, and the greatest cornering force can be observed, as shown in Figs 8a and 8b.

5.2.3 Current remarks

When a vehicle negotiates a constant radius turn, the favourable full control modes will be those choosing two steering angles and only one tractive force provided by the single wheel as the control parameters, such as mode Q9. Using only one steering angle, in modes Q1 to Q6, demands a greater total tractive force than modes Q7 to Q9. The total cornering forces in modes Q7, Q8 and Q1 to Q3 are about the same, whereas mode Q6, which uses the rear steering angle, single-wheel tractive force, and inside wheel tractive force as the control parameters contribute the highest total tractive force and cornering force.

With respect to their active suspension forces, the three-wheeled vehicles 2F1R and 1F2R exhibit no differences from an energy-saving point of view in a constant radius turn.

6 CONCLUSIONS

In this study, various full control modes for controlling three-wheeled vehicle body sideslip angle and body motion are presented by means of a six-degree-of-freedom vehicle model. Evaluation criteria, such as the sum of total tractive forces, total cornering forces and total active suspension forces, have been developed for comparing the different performances of these nine control modes. Through the discussion and numerical simulation, the favourable control modes for zero body sideslip angle and zero body motions control in various driving scenarios have been found. The conclusions are as follows:

1. In the straight-line run, the full control modes choosing two tractive forces and only one steering angle or choosing two steering angles and the tractive force provided by the singled wheel as control parameters are preferable, because there are no cornering forces.
2. In the constant radius turn, the full control modes choosing two steering angles and tractive force provided by the singled wheel as control parameters are preferable, because of the lower tractive and cornering forces.
3. With respect to active suspension forces, there is no difference between a 2F1R or 1F2R three-wheeled vehicle.

REFERENCES

1 **Yu, C. C.** and **Liu, T.** Strategies on the full control of vehicle handling. *Bull. Coll. Engng, NTU*, October 1997, **71**, 91–106.
2 **Hurdwell, R.** and **Pilling, M. J.** Active suspension and rear wheel steering make powerful research and development tools. *SAE Trans.*, 1993, **101**, 67–77.

3 **Iguchi, M.** A new concept of vehicle dynamics based on active control. *Jap. Soc. Mech. Engrs Int. J., Ser. III*, 1988, **31**(1), 1–7.

4 **Sharp, R.** and **Crolla, D.** Road vehicle suspension system design—a review. *Veh. System Dynamics*, 1987, **16**(3), 167–192.

5 **Naohiro, F. Y., Shoichi, S., Hideo, T.** and **Yoshinobu, M.** A review of four-wheel steering studies from the viewpoint of vehicle dynamics and control. *Veh. System Dynamics*, 1989, **18**(1–3), 151–186.

6 **Sano, S., Furukawa, Y.** and **Shiraishi, S.** Four wheel steering system with rear wheel steer angle controlled as a function of steering wheel angle. *SAE Trans.*, 1986, **94**, 3880–3893.

7 **Dixon, J. C.** *Tyres, Suspension and Handling*, 1st edition, 1991, pp. 187–249 (Cambridge University Press, Cambridge).

8 **Wong, J. Y.** *Theory of Ground Vehicles*, 2nd edition, 1993, pp. 281–309 (John Wiley, New York).

9 **Masaki, Y.** Active control strategy for improved handling and stability. *SAE Trans.*, 1991, **99**, 1638–1648.

10 **Abe, M.** Handling characteristics of four wheel active steering vehicles over full maneuvering range of lateral and longitudinal acceleration. In Eleventh IAVSD Symposium, 1989, pp. 1–14.

11 **Matsumoto, N.** and **Tomizuka, M.** Vehicle lateral velocity and yaw rate control with two independent control inputs. *Trans. ASME, J. Dynamic Systems, Measmt Control*, 1992, **114**(4), 606–613.